

Study of Structural Properties of Solar Energy Material $\text{CH}_3\text{NH}_3\text{PbX}_3$ ($\text{X} = \text{I}, \text{Br}$ and Cl) Perovskites and its Mixed Halides Using Density Functional Theory

Sachin Sharma¹, Sanjay Prakash Kaushik², Ram-Krishna Thakur³,
Vivek Kumar Shukla^{1*}

¹Department of Applied Physics, Gautam Buddha University, Greater Noida,
Gautam Budh Nagar (U.P.) India, 201312

²Department of Science, State Council for Educational Research & Training,
Gurugram Haryana-122001, India

³Jaipur National University, Rajasthan -302017, India

*CORRESPONDING AUTHOR:

Vivek Kumar Shukla
Email: vkshuk@gmail.com

ISSN : 2382-5359(Online),
1994-1412(Print)

DOI:

<https://doi.org/10.3126/njst.v21i2.62360>



Date of Submission: 14/11/2022

Date of Acceptance: 24/02/2023

Copyright: The Author(s) 2022. This is an open access article under the [CC BY](#) license.



ABSTRACT

The present study has explored the electronic properties of Organic-inorganic mixed halide-based perovskites using density functional theory. The Quantum Espresso simulation package with PBE parameterization within the generalized gradient approximation (GGA) has been used in this work. The findings reveal that the addition of halogens (bromide and chlorine) to compound $\text{CH}_3\text{NH}_3\text{PbI}_3$ for all the possible substituted halides may cause the shifting of energy bands in the band structure and thus change the bandgap. Hence, this calculation may be used to design perovskite solar cell material with varied electronic structure.

Keywords: Density Functional Theory, Local Density approximation, Perdew-Burke-Ernzerh, Generalized Gradient Approximation, Projected Augmented Wave, Ultra soft Pseudopotentials

1. INTRODUCTION

Organic-inorganic halide-based perovskites solar cells have shown a bright scope in energy generation in the last few years. Perovskite photovoltaics has been the center of attraction for the scientific community because of their exceptional light-absorbing properties (Petrovic *et al.* 2015). Organic-inorganic metal halide perovskites are demonstrated to be promising materials in a variety of optoelectronic applications including photodetection, energy harvesting, and light-emitting devices (Sun *et al.* 2018). Organic-inorganic hybrid semiconductors show promising electronic and optical properties (Papavassiliou 1977). Recently, Methyl ammonium lead halide perovskite $\text{CH}_3\text{NH}_3\text{PbX}_3$ (X = I, Br, Cl) and its mixed halides ($\text{CH}_3\text{NH}_3\text{PbI}_3$, $\text{CH}_3\text{NH}_3\text{PbI}_2\text{Cl}$, $\text{CH}_3\text{NH}_3\text{PbCl}_2$, $\text{CH}_3\text{NH}_3\text{PbCl}_3$, $\text{CH}_3\text{NH}_3\text{PbBr}_3$, $\text{CH}_3\text{NH}_3\text{PbBr}_2\text{Cl}$, $\text{CH}_3\text{NH}_3\text{BrCl}_2$, $\text{CH}_3\text{NH}_3\text{PbBr}_2\text{I}$, $\text{CH}_3\text{NH}_3\text{BrI}_2$) have emerged as important optoelectronic materials. With the emanation of Methyl ammonium lead halide perovskite $\text{CH}_3\text{NH}_3\text{PbX}_3$, it becomes easy to fabricate solar cells cheaply from the liquid phase (Boix *et al.* 2014), and increment in the power conversion efficiencies (PCEs) from 3.8% in 2009 (Loi & Hummelen 2013) to about 22% in 2019 has been observed. The first effectiveness of $\text{CH}_3\text{NH}_3\text{PbI}_3$ for visible light conversion with photo-voltages approximately equal to 1.0 eV was reported by researchers (Kojima *et al.* 2009). Hybrid organic and inorganic perovskite has a vast variety of composed materials that is organic molecules and metal and halide ions that increase the scope of work in this field. Other species with oxidation states similar to their counterpart can replace the metal ions and halide ions. Replacements of Pb^{2+} with Sn^{2+} have shown quite a positive result except for the issue of stability (Noel *et al.* 2014; Hao *et al.* 2014). Moreover this, partial replacement of Pb^{2+} with Sn^{2+} , Sr^{2+} , Cr^{2+} , and Cd^{2+} perovskites has been explored theoretically and experimentally (Hao *et al.* 2014; Mosconi *et al.* 2015; Giorgi *et al.* 2015; Sun *et al.* 2015). Replacing halogen in partial amounts also suggests new hopes in solving the stability problem of halides-based perovskites, e.g., partially replacing I with Cl and Br (Jong *et al.* 2016). Replacement of halides gives rise to change in band structure. Therefore,

studies on mixed halides-based perovskites become important. Structural, electronic, and optical parameters for cubic perovskite BaCeO_3 were calculated, and its semiconducting nature was established (Murali *et al.* 2021). The synthesis, followed by an investigation of structural and electric properties for $\text{Bi}_{1-x}\text{Ca}_x\text{FeO}_3$ was performed, and the rhombohedral structure was confirmed (Sravani *et al.* 2022).

2. COMPUTATIONAL DETAILS

The plane-wave QUANTUM ESPRESSO (QE) package (Giannozzi *et al.* 2009) with the Perdew-Burke-Ernzerh (PBE) parameterization for the exchange-correlation functional within the generalized gradient approximation (GGA), was used for density functional theory calculation. The pseudopotential technique has proven to be dynamic and instrumental tool for studying different materials of electronic and structural properties (Martin 2009). GGA functionals are non-local functional in the literature. These functionals are ‘non-local’ is supported by the fact that these functionals go beyond the ‘local’ density approximation and that accounts for the inhomogeneity of the real density. GGA seeks to improve the accuracy of the local spin density approximation in electronic structure calculations (Perdew *et al.* 1996). The electron-ion interactions were set up using Projected Augmented Wave (PAW) pseudopotentials and the kinetic energy cut-off limit for wave functions was set to 200 eV. The projected wave function was proposed after the Ultra soft Pseudopotentials (USPP) method was initially used. Compared to the USPP, the PAW method helps from a cleaner link with the underlying all-electron treatment, making it more accurate than the USPP method. PAW method provides more reliability in the case of magnetic systems. However, the generation of US pseudopotential is more difficult than the generation of PAW atomic data (Audouze *et al.* 2008). The geometry optimization and the band structure were calculated by selecting a K-point mesh of $8 \times 8 \times 8$ centered at the Γ point. The optimization of the atomic positions and lattice vectors has been done as per the guidance of the atomic forces. As per the norm, the calculated force

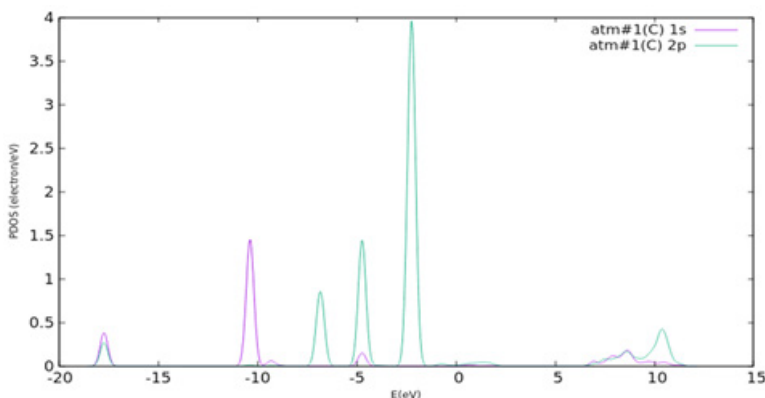
on each atom must be smaller than 0.02 eV/\AA . The convergent threshold for self-consistent-field iteration is 10^{-8} eV . Apart from, partially replacing I with Cl and Br, similar calculations have also been done by partially replacing Br and Cl with each other. Overall, calculations for nine possible structures have been done and reported here.

3. RESULTS AND DISCUSSION

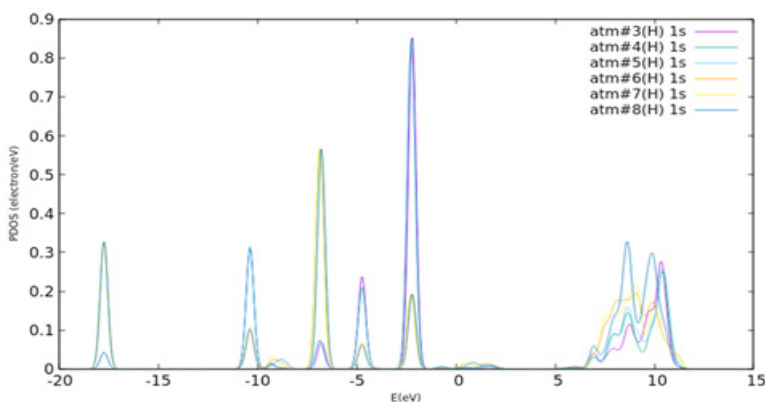
Calculations for relaxed structures of all nine combinations of sole and mixed halides perovskites have been performed, which results in the band structure, band gap, lattice parameters, and projected density of the states (PDOS). The

investigation of the projected density of the states and band structure results revealed that all nine $\text{CH}_3\text{NH}_3\text{PbX}_3$ sole and mixed halide perovskite compounds exhibit different electronic properties. The density of states and stability for a few II-VI semiconducting materials have already been reported in our earlier published work (Singh *et al.* 2020; Kaushik *et al.* 2020). Our group has also studied the electronic structure of PbTiO_3 (Shukla 2018). In this work, the projected density of the states and band structures of $\text{CH}_3\text{NH}_3\text{PbI}_2\text{Cl}$ have been shown and discussed for reference. The main results for the other eight compounds are also reported and compared.

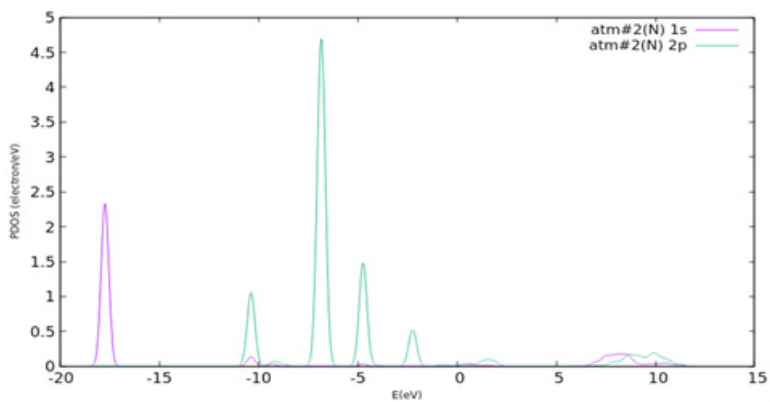
The calculated projected density of the states for each atom present in the structure of $\text{CH}_3\text{NH}_3\text{PbI}_2\text{Cl}$ is shown in Fig. 1.



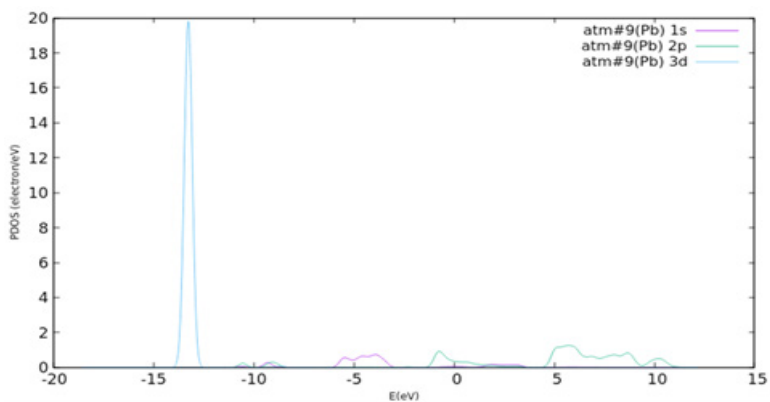
(a) Projected density of the state of C



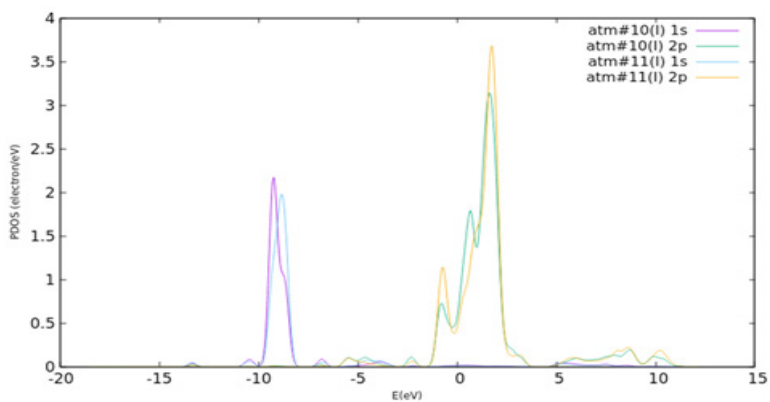
(b) Projected density of the state of H



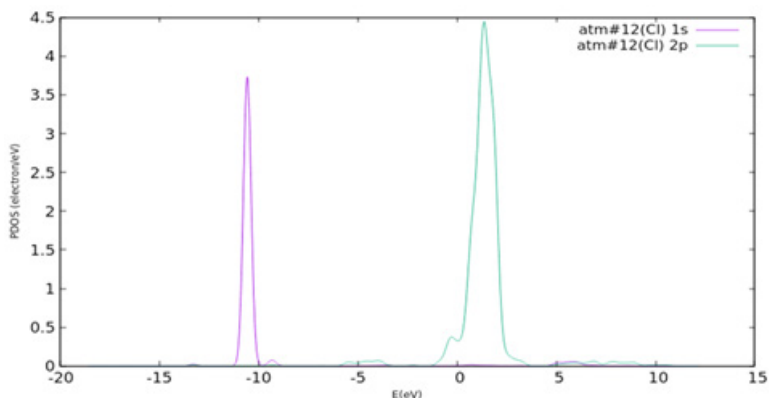
(c) Projected density of the state of N



(d) Projected density of the state of Pb



(e) Projected density of the state of I



(f) Projected density of the state of Cl

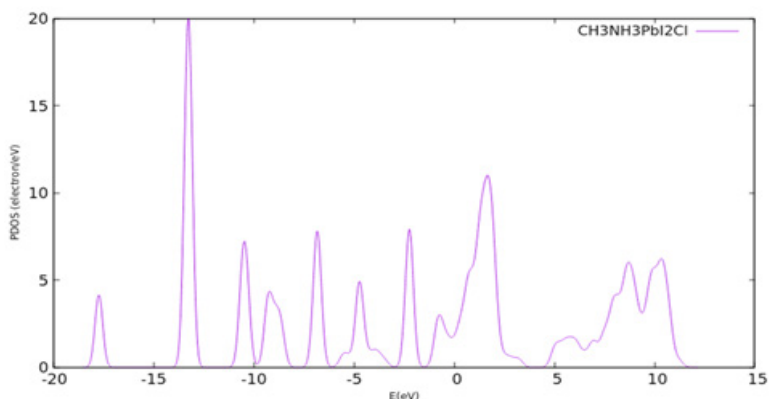
(g) Projected density of the state of $\text{CH}_3\text{NH}_3\text{PbI}_2\text{Cl}$

Fig.1. Calculated projected density of state plots for each atom of $\text{CH}_3\text{NH}_3\text{PbI}_2\text{Cl}$. (a) Projected density of the state of C (b) Projected density of the state of H (c) Projected density of the state of N (d) Projected density of the state of Pb (e) Projected density of the state of I (f) Projected density of state of Cl (g) Total projected density of the state of $\text{CH}_3\text{NH}_3\text{PbI}_2\text{Cl}$.

The calculated projected density of the states for $\text{CH}_3\text{NH}_3\text{PbI}_2\text{Cl}$ and its atoms C, N, H, Pb, I, and Cl are shown in Figure 1. The valence band is primarily the anti-bonding part of the hybridization between C 2p and N 2p, Pb 3d and Cl 1s states. At the same time the conduction band is relatively a nonbonding state prevailed by the Pb 2p and Cl 2p states. The electronic levels of rest states of atoms are placed deep in

the conduction band and valence band, without contributing to the states close to the Fermi level. The highest value of the calculated projected density of the states for $\text{CH}_3\text{NH}_3\text{PbI}_2\text{Cl}$ and Pb 3d is 20 electrons/eV at -13.90 eV.

The results of the relaxed structures give information about the electronic properties of the $\text{CH}_3\text{NH}_3\text{PbI}_2\text{Cl}$ compound, along with band structure, band gap, and density of the states. The investigations suggest that the $\text{CH}_3\text{NH}_3\text{PbI}_2\text{Cl}$ compound has a direct band gap at point R (0.016, 0.016, 0.016). The band structure for the $\text{CH}_3\text{NH}_3\text{PbI}_2\text{Cl}$ compound is shown in Fig. 2. The result shows that the electric-dipole transition at R from valence band maximum (VBM) to conduction band minimum (CBM) is granted, which gives an optical band gap of 1.90 eV.

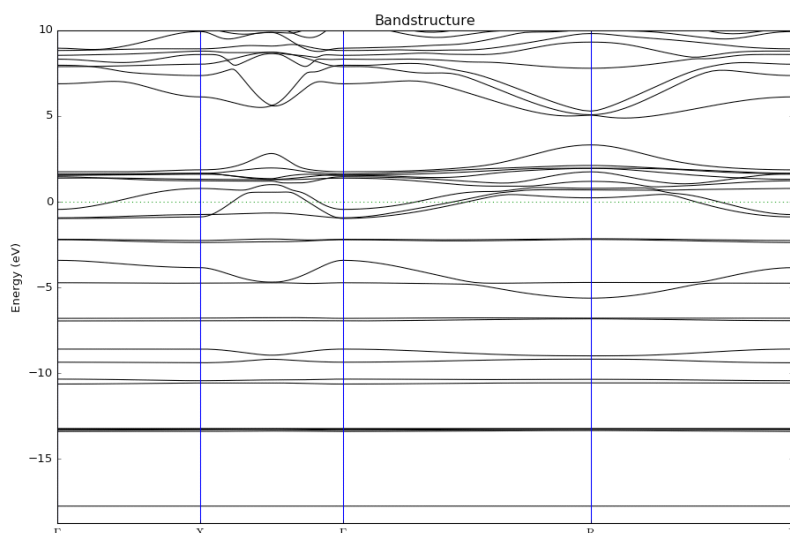


Fig. 2. Calculated band structure for $\text{CH}_3\text{NH}_3\text{PbI}_2\text{Cl}$ using PBE functional when the valence bands moved down and the conduction bands moved up. The zero is at the valence band maximum.

Results for band gap and lattice parameters for all the possible structures in Organometallic halides, which are partially substituted with halogens, are shown in Table 1.

Table 1: Calculated band gap and lattice parameters for all the possible Organometallic halide structures studied in the present work.

Structures	a (Å)	b (Å)	c (Å)	E_g (eV)
$\text{CH}_3\text{NH}_3\text{I}_3$	6.26	6.25	6.25	1.14
$\text{CH}_3\text{NH}_3\text{I}_2\text{Cl}$	6.26	6.25	6.25	1.9
$\text{CH}_3\text{NH}_3\text{ICl}_2$	6.13	5.77	5.7	1.82
$\text{CH}_3\text{NH}_3\text{Cl}_3$	5.59	5.45	5.5	2.2
$\text{CH}_3\text{NH}_3\text{Br}_3$	6.01	6.02	5.96	1.89
$\text{CH}_3\text{NH}_3\text{Br}_2\text{Cl}$	5.88	5.88	5.9	1.88
$\text{CH}_3\text{NH}_3\text{BrCl}_2$	5.71	5.7	5.89	2.2
$\text{CH}_3\text{NH}_3\text{Br}_2\text{I}$	5.81	5.85	6.2	1.17
$\text{CH}_3\text{NH}_3\text{BrI}_2$	6.19	5.86	6.04	1.05

The organometallic halide perovskites $\text{CH}_3\text{NH}_3\text{Cl}_3$, $\text{CH}_3\text{NH}_3\text{Br}_3$, and $\text{CH}_3\text{NH}_3\text{I}_3$ have a band gap of 2.20, 1.89, and 1.14 eV respectively. Hence, the value of the band gap decreases as X varies from the smaller to the larger size of an attached atom. Also, the larger the size of the attached halogen atom in $\text{CH}_3\text{NH}_3\text{X}_3$, the larger will be the lattice parameters. The size of the Chlorine atom is less than the Bromine atom which is smaller than the Iodine atom.

The partial substitution of chlorine atoms in $\text{CH}_3\text{NH}_3\text{PbI}_{3-x}\text{Cl}_x$ ($x=1,2,3$) increases the band gap and decreases lattice parameters. Partial substitution of bromine atoms in $\text{CH}_3\text{NH}_3\text{PbBr}_{3-x}\text{Cl}_x$ ($x=1,2,3$) results in an increase or decrease in the band gap and a decrease in lattice parameters. The values of the change in these parameters depend on the number of Br atoms substituted.

To validate our results we have compared these results with the literature, as shown in Table 2 to Table 10.

Table 2: Calculated structural properties and PBE band gap of CH₃NH₃PbI₃ for cubic structure unit cell.

CH ₃ NH ₃ PbI ₃	Mohebpour <i>et al</i> 2016 (PBE)	Menendez -Proupin <i>et al</i> 2014 (PBE) (PAW)	Kumar, S. 2018 (PBE) (USPP)	Our results (PBE) (PAW)	Structure (Space Group)
a	6.31	6.46	6.18	6.26	Cubic
b	6.31	6.46	6.18	6.25	(Pm3m)
c	6.31	6.46	6.18	6.25	
E _g	-	1.71	1.14	1.14	

Table 3: Calculated structural properties and PBE band gap of CH₃NH₃PbI₂Cl for cubic structure unit cell.

CH ₃ NH ₃ PbI ₂ Cl ₃	Mohebpour <i>et al</i> 2016 (PBE)	Kiong <i>et al</i> 2017 (PBE)	Our results (PBE) (PAW)	Structure (Space group)
a	6.31	6.46	6.26	Cubic
b	6.31	6.46	6.25	(Pm3m)
c	6.32	6.46	6.25	
E _g	-	1.597	1.9	

Table 4: Calculated structural properties and PBE band gap of CH₃NH₃PbICl₂ for cubic structure unit cell.

CH ₃ NH ₃ PbICl ₂	Mohebpour <i>et al</i> 2016 (PBE)	Kiong <i>et al</i> 2017 (PBE)	Our results (PBE) (PAW)	Structure (Space group)
a	6.31	-	6.13	Cubic
b	6.31	-	5.77	(Pm3m)
c	6.32	-	5.7	
E _g	-	1.59	1.821	

Table 5: Calculated structural properties and PBE band gap of CH₃NH₃PbCl₃ for cubic structure unit cell.

CH ₃ NH ₃ PbCl ₃	Mohebpour <i>et al</i> 2016 (PBE)	Ye <i>et al</i> 2015 (PBE)	Kumar, S. 2018 (PBE) (USPP)	Our results (PBE) (PAW)	Structure (Space Group)
a	5.68	5.91	5.58	5.59	Cubic
b	5.61	5.91	5.58	5.45	(Pm3m)
c	5.73	5.91	5.58	5.5	
E _g	-	2.36	2.85	2.2	

Table 6: Calculated structural properties and PBE band gap of $\text{CH}_3\text{NH}_3\text{PbBr}_3$ for cubic structure unit cell.

$\text{CH}_3\text{NH}_3\text{PbBr}_3$	Ye <i>et al</i> 2015 (PBE)	Mohebpour <i>et al</i> 2016 (PBE)	Kumar, S. 2018 (PBE) (USPP)	Our results (PBE) (PAW)	Structure (Space Group)
a	6.02	5.93	5.84	6.01	Cubic
b	6.02	5.93	5.84	6.02	(Pm3m)
c	6.02	5.93	5.84	5.96	
Eg	1.71	2.23	2.286	1.89	

Table 7: Calculated structural properties and PBE band gap of $\text{CH}_3\text{NH}_3\text{PbBr}_2\text{Cl}$ for cubic structure unit cell.

$\text{CH}_3\text{NH}_3\text{PbBr}_2\text{Cl}$	Mohebpour <i>et al</i> 2016 (PBE) (PAW)	Our results (PBE) (PAW)	Structure (Space Group)
a	5.88	5.88	Cubic
b	5.88	5.88	(Pm3m)
c	5.88	5.9	
Eg	2.42	1.88	

Table 8: Calculated structural properties and PBE band gap of $\text{CH}_3\text{NH}_3\text{PbBr}_3$ for cubic structure unit cell.

$\text{CH}_3\text{NH}_3\text{PbBrCl}_3$	Mohebpour <i>et al</i> 2016 (PBE) (PAW)	Our results (PBE) (PAW)	Structure (Space group)
a	5.78	5.71	Cubic
b	5.78	5.7	(Pm3m)
c	5.78	5.89	
Eg	2.9	2.2	

Table 9: Calculated structural properties and PBE band gap of $\text{CH}_3\text{NH}_3\text{PbBr}_2\text{I}$ for cubic structure unit cell.

$\text{CH}_3\text{NH}_3\text{PbBr}_2\text{I}$	Mohebpour <i>et al</i> 2018 (PBE)	Our results (PBE) (PAW)	Structure (Space Group)
a	5.95	5.81	Cubic
b	5.95	5.85	(Pm3m)
c	6.3	6.2	
Eg	1.59	1.17	

Table 10: Calculated structural properties and PBE band gap of $\text{CH}_3\text{NH}_3\text{PbBrI}_2$ for cubic structure unit cell.

$\text{CH}_3\text{NH}_3\text{PbBrI}_2$	Mohebpour <i>et al</i> 2018 (PBE)	Our results (PBE) (PAW)	Structure (Space Group)
a	6.3	6.19	Cubic
b	5.93	5.86	(Pm3m)
c	6.3	6.04	
Eg	1.47	1.05	

The tables show theoretical calculations on structural and electronic parameters of $\text{CH}_3\text{NH}_3\text{X}_3$ perovskites. It is also important to validate the theoretical results with the experimental one for applications. In this direction, Dimesso *et al.* (2014) synthesized the materials, performed optical experiments and found $\text{CH}_3\text{NH}_3\text{X}_3$ material as direct-gap semiconductors with energy band gaps of 1.53 eV for $X = \text{I}$, 2.20 eV for $X = \text{Br}$, and 3.00 eV for $X = \text{Cl}$, respectively, at room temperature. It has been observed that the theoretically calculated value of energy band gaps (see E_g in the above tables) are slightly higher than the experimental values for these materials. It should be noted that the value of the band gap decreases as X varies from the smaller to the larger size of an attached atom, which agrees with our results reported here in this work.

4. CONCLUSION

The electronic properties of $\text{CH}_3\text{NH}_3\text{PbX}_3$ ($X = \text{I}, \text{Br}, \text{Cl}$) and its mixed halides have been studied. The structures lattice parameters and band gap have been calculated using Quantum Espresso. The findings for projected density of the states (PDOS) and band structure reveal that all the nine $\text{CH}_3\text{NH}_3\text{PbX}_3$ sole and mixed halide perovskite compounds exhibit different electronic properties. These finding may further be used for optimizing the structural parameters of such perovskite materials for solar cell and other various device applications.

ACKNOWLEDGEMENT

The authors acknowledge Quantum ESPRESSO Foundation for offering a free service for simulation and modeling.

REFERENCES

- Audouze, C., F. Jollet, M. Torrent, and X. Gonze, 2008. Comparison between projector augmented-wave and ultrasoft pseudopotential formalisms at the density-functional perturbation theory level. *Physical Review B*, 78(3), 035105.
- Boix, P. P., K. Nonomura, N. Mathews, and S. G. Mhaisalkar, 2014. Current progress and future perspectives for organic/inorganic perovskite solar cells. *Materials today*, 17(1), 16-23.
- Dimesso, L., M. Dimamay, M. Hamburger, and W. Jaegermann, 2014. Properties of $\text{CH}_3\text{NH}_3\text{PbX}_3$ ($X = \text{I}, \text{Br}, \text{Cl}$) powders as precursors for organic/inorganic solar cells. *Chemistry of Materials*, 26(23), 6762-6770.
- Giannozzi, P., S. Baroni, N. Bonini, M. Calandra, R. Car, C. Cavazzoni, and R. M. Wentzcovitch, 2009. QUANTUM ESPRESSO: a modular and open-source software project for quantum simulations of materials. *Journal of physics: Condensed matter*, 21(39), 395502.
- Giorgi, G., and K. Yamashita, 2015. Alternative, lead-free, hybrid organic-inorganic perovskites for solar applications: A DFT analysis. *Chemistry Letters*, 44(6), 826-828.
- Hao, F., C. C. Stoumpos, D. H. Cao, R. P. Chang, and M. G. Kanatzidis, 2014. Lead-free solid-state organic-inorganic halide perovskite solar cells. *Nature photonics*, 8(6), 489-494.
- Hao, F., C. C. Stoumpos, R. P. Chang, and M. G. Kanatzidis, 2014. Anomalous band gap behavior in mixed Sn and Pb perovskites enables broadening of absorption spectrum in solar cells. *Journal of the American Chemical Society*, 136(22), 8094-8099.
- Jong, U. G., C. J. Yu, J. S. Ri, N. H. Kim, and G. C. Ri, 2016. Influence of halide composition on the structural, electronic, and optical properties of mixed $\text{CH}_3\text{NH}_3\text{Pb}(\text{I}1-x\text{Br}x)_3$ perovskites calculated using the virtual crystal approximation method. *Physical review B*, 94(12), 125139.
- Kaushik, S. P., S. Singh, and R. K. Thakur, 2020. First Principles Study of Structural Stability and Electronic Properties of CdTe Nanowires. *Journal of Computational and Theoretical Nanoscience*, 17(12), 5210-5214.
- Kiong, L. J., and J. Rajan, 2017. Effect of Halogen Substitution on the Absorption and Emission Profile of Organometallic Perovskites. In *MATEC Web of Conferences* (Vol. 131, p. 03001). EDP Sciences.
- Kojima, A., K. Teshima, Y. Shirai, and T. Miyasaka, 2009. Organometal halide perovskites as visible-light sensitizers for photovoltaic cells. *Journal of the american chemical society*, 131(17), 6050-6051.

- Kumar, S., 2018. Study of Mixed Perovskites organometallic halides using Density Functional Theory. MS Dissertation. Department of Applied Physics, Gautam Buddha University, Greater Noida, India.
- Loi, M. A., and J. C. Hummelen, 2013. Hybrid solar cells: perovskites under the sun. *Nature materials*, 12(12), 1087-1089.
- Martin, R. M., 2009. *Electronic structure: basic theory and practical methods*. Cambridge university press.
- Menéndez-Proupin, E., P. Palacios, P. Wahnón, and J. C. Conesa, 2014. Self-consistent relativistic band structure of the $\text{CH}_3\text{NH}_3\text{PbI}_3$ perovskite. *Physical Review B*, 90(4), 045207.
- Mohebpour, M. A., M. Saffari, H. R. Soleimani, and M. B. Tagani, 2018. High performance of mixed halide perovskite solar cells: Role of halogen atom and plasmonic nanoparticles on the ideal current density of cell. *Physica E: Low-dimensional Systems and Nanostructures*, 97, 282-289.
- Mosconi, E., P. Umari, and F. De Angelis, 2015. Electronic and optical properties of mixed Sn–Pb organohalide perovskites: a first principles investigation. *Journal of Materials Chemistry A*, 3(17), 9208-9215.
- Murali, N., K. E. Babu, P. S. Tadesse, A. Ramakrishna, D. Parajuli, Pramila, R. P. N., ... and V. Veeraiah, 2021. Theoretical investigation of structural, electronic, dielectric and optical characteristics of cubic perovskite BaCeO_3 . *Processing and Application of Ceramics*, 15(4), 351-356.
- Noel, N. K., S. D. Stranks, A. Abate, C. Wehrenfennig, S. Guarnera, Haghighirad, A. A., ... & H. J. Snaith, 2014. Lead-free organic–inorganic tin halide perovskites for photovoltaic applications. *Energy & Environmental Science*, 7(9), 3061-3068.
- Papavassiliou, G. C., 1997. Three-and low-dimensional inorganic semiconductors. *Progress in Solid State Chemistry*, 25(3-4), 125-270.
- Perdew, J. P., K. Burke, and M. Ernzerhof, 1996. Generalized gradient approximation made simple. *Physical review letters*, 77(18), 3865.
- Petrović, M., V. Chellappan, and S. Ramakrishna, 2015. Perovskites: solar cells & engineering applications—materials and device developments. *Solar Energy*, 122, 678-699.
- Prakash, K. S., S. Satyendra, and K. Ram-Krishna, 2020. Stability and electronic properties of ZnSe nanowires: An ab initio approach. *Наносистемы: физика, химия, математика*, 11(5), 546-552.
- Saffari, M., M. A. Mohebpour, H. R. Soleimani, and M. B. Tagani, 2017. DFT analysis and FDTD simulation of $\text{CH}_3\text{NH}_3\text{PbI}_3\text{-xCl}_x$ mixed halide perovskite solar cells: role of halide mixing and light trapping technique. *Journal of Physics D: Applied Physics*, 50(41), 415501.
- Shukla, V. K., 2018. Electronic structure of PbTiO_3 perovskite based on density functional calculation. In *AIP Conference Proceedings* (Vol. 1953, No. 1, p. 110035). AIP Publishing LLC.
- Singh, S., and S. P. Kaushik, 2020. Ab Initio Study of Electronic Properties of Cadmium Sulphide Nanowires. *Journal of Computational and Theoretical Nanoscience*, 17(2-3), 546-551.
- Sravani, G. M., N. Murali, B. C. Sekhar, B. Dhanalakshmi, D. Parajuli, T. G. Naidu, and K. Samatha, 2022. Structural and electrical properties of Ca doped BiFeO_3 multiferroic nanomaterials prepared by sol-gel auto-combustion method. *Journal of the Indian Chemical Society*, 99(6), 100465.
- Sun, J., J. Wu, X. Tong, F. Lin, Y. Wang, and Z. M. Wang, 2018. Organic/inorganic metal halide perovskite optoelectronic devices beyond solar cells. *Advanced Science*, 5(5), 1700780.
- Sun, Y. Y., M. L. Agiorgousis, P. Zhang, and S. Zhang, 2015. Chalcogenide perovskites for photovoltaics. *Nano letters*, 15(1), 581-585.
- Yuan, Y., R. Xu, H. T. Xu, F. Hong, F. Xu, and L. J. Wang, 2015. Nature of the band gap of halide perovskites ABX_3 ($\text{A} = \text{CH}_3\text{NH}_3, \text{Cs}$; $\text{B} = \text{Sn, Pb}$; $\text{X} = \text{Cl, Br, I}$): First-principles calculations. *Chinese Physics B*, 24(11), 116302.